Taylor & Francis
Taylor & Francis Group

Fabrication of Superhydrophobic Zinc Stearate Hierarchical Surfaces from Different Precursors

Edna Richard, C. Anandan, and S. T. Aruna

Surface Engineering Division, CSIR-National Aerospace Laboratories, HAL Airport Road, Bangalore, India

The fabrication of zinc stearate superhydrophobic hierarchical surfaces from two precursors by a simple wet chemical route and its wettability is reported. The zinc stearate coatings were prepared from a single pot using ethanolic solutions of zinc acetate/zinc nitrate and stearic acid. The coatings were characterized by X-ray diffraction, X-ray photoelectron spectroscopy, Fourier-transform infrared spectroscopy, field emission scanning electron microscopy, water contact angle, and sliding angle measurements. The coatings obtained from zinc acetate precursor showed superhydrophobicity (WCA >150°) even at lower precursor concentrations. The morphology of the coatings varied with the nature as well as the concentration of the precursors.

Keywords Acetate; Angle; Contact; Microstructure; Morphology; Nitrate; Precursors; Roughness; Sliding; Stearate; Superhydrophobic.

INTRODUCTION

Superhydophobicity observed in biological structures such as lotus leaf has attracted researchers due to their broad range of applications extending from self-cleaning materials to microfluidic devices [1–5]. Generally, surfaces with a water contact angle (WCA) greater than 150° and sliding angle (SA) less than 10° are called superhydrophobic surfaces. Water drops on such surfaces effortlessly roll off, washing away dirt completely and thus realizing the "lotus effect." This effect is attributed to the combination of micro-nano surface roughness and low surface energy which is based on the studies carried out by Neinhuis and Barthlott on the lotus leaf [6]. Accordingly, two strategies have been developed to create artificial superhydrophobic surfaces: (i) create a rough surface and modify it with a low surface energy material and (ii) roughen the surface of hydrophobic material and make it superhydrophobic. A large number of papers on superhydrophobic surfaces from metals, metal oxides, and polymers have been reported [7–12].

Zinc stearates are well-known lubricant additives that improve pigment or filler dispersion in hydrophobic plastics media [13]. Zinc stearate also finds application as an acid scavenger and processing aid in certain polyolefin applications. Zinc stearates are being used in the paint and coatings industry for pigment suspension, and also as hydrophobic agents for plasters. Recently, superhydrophobic zinc oxide surfaces have been modified with stearic acid. Zinc oxide stearate superhydrophobic surface has been fabricated by modifying solution combustion synthesized ZnO with stearic acid [14]. A layer of lamellar superhydrophobic zinc stearate coating on a wood surface through a wet chemical process has been reported [15]. Gurav et al. studied the static and dynamic wettability of zinc oxide nanorods modified with different concentrations of stearic acid [16].

In this article, we report the preparation of zinc stearate superhydrophobic surfaces starting from zinc precursors like zinc acetate and zinc nitrate instead of ZnO. The effect of different concentrations of the zinc precursors on the microstructure and wettability of the surfaces has been studied.

MATERIALS AND METHODS

Zinc acetate, zinc nitrate, and stearic acid were purchased from Loba Chemie (Mumbai, India). Ammonium hydroxide and ethanol were purchased from Merck. A definite amount of zinc acetate/or zinc nitrate was dissolved in 40 mL ethanol followed by the addition of ammonium hydroxide to obtain 0.01, 0.025, 0.1, 0.2, and 0.3 M solutions. Then, 5 mL of 5 wt% stearic acid (designated as SAc) solution in ethanol was added to the above solution to obtain the final precursor solution (designated as ZnA for zinc acetate and ZnN for zinc nitrate precursor). During the addition of ammonium hydroxide, the solution which was milky in the beginning turned clear due to the formation of zinc amino complex. The precursor solution was then heated to 70°C and maintained at that temperature for about 45 min in an open beaker. The pH of the precursor solution at the start of the experiment was 10 which reduced to 8 after 45 min. At this stage, the precursor solution was uniformly spread over a cleaned glass substrate using a glass rod to obtain the coating. The as-prepared coatings were dried at ambient conditions.

Contact angle analyzer (model Phoenix 300 Plus, M/s Surface Electro Optics) was used for measuring static

---

Address correspondence to S. T. Aruna, Surface Engineering Division, CSIR-National Aerospace Laboratories, HAL Airport Road, P.B. No. 1779, Bangalore 560017, India; E-mail: aruna_reddy@nal.res.in

Color versions of one or more of the figures in the article can be found online at www.tandfonline.com/lmmp.

WCA of the coatings using 8 μL as the drop volume. Tangent fitting mode was used in this instrument for the determination of WCA. Five measurements of WCA on the coating were taken, and the mean value has been reported. A simple in-house fabricated setup was used for measuring SA—the angle at which the drop slides was measured by means of a protractor attached to the setup. The crystalline nature of the coatings was examined by X-ray diffraction (XRD) technique using powder X-ray diffractometer (Bruker D-8 Advanced) with Cu Kα radiation of wavelength 0.154 nm. Surface morphology of the coatings was examined using field emission scanning electron microscope (FESEM, Carl Zeiss). X-ray photoelectron spectra (XPS) of the coatings were obtained using Specs, surface nanoanalysis. Fourier-transform infrared (FTIR) spectra were recorded on Bruker Alpha-P spectrometer.

RESULTS AND DISCUSSION

Figure 1 shows the XRD patterns of the powders obtained by stripping off the coatings prepared from 0.3 M ZnA and ZnN precursors. Five XRD peaks were detected corresponding to Bragg angles 6.53°, 8.6°, 10.6°, 19.5°, and 23.6°, respectively. All the diffraction peaks are indexed to zinc stearate, which is in accordance with the JCPDS file No. 05-0079.

XPS analysis was employed to understand the chemical composition and chemical state of the elements present on the surfaces prepared from two different precursors, i.e., ZnN and ZnA at higher concentration (0.3 M). The broad survey scan XPS spectra of the coatings (Fig. 2) prepared from both the precursors show the presence of Zn, C, and O. The peaks observed at binding energies of 1020.5 and 1043.4 eV correspond to $Zn2p_{3/2}$ and $Zn2p_{1/2}$ states. The peak at 532.2 eV confirms O–Zn bonding state. The C1s peak at 284.0 eV arises due to stearic acid modification [16]. From the XPS study, it is evident that irrespective of the precursors used for preparing zinc stearate surfaces, the chemical composition of the surface remains unaltered.
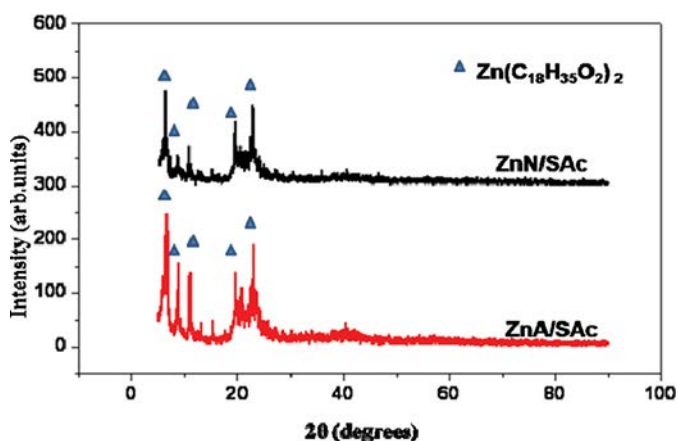
Irrespective of the precursors used, the FTIR spectra of zinc stearate coatings were similar (Fig. 3). The bands observed at 2850 and 2920 cm^{-1} correspond to the symmetric and asymmetric stretching modes of zinc stearate ($C_{36}H_{70}O_4Zn$). The band observed at 1541 cm^{-1} is attributed to asymmetric stretching of COO$^-$. The band corresponding to unreacted stearic acid (1704 cm^{-1}) was not observed. The observed bands match well with the reported literature [14].

The surface wettability of the coatings developed from ZnN and ZnA precursors was evaluated based on WCA and SA measurements (Table 1). The coatings prepared with ZnA and ZnN precursors without using stearic acid were hydrophilic with WCA of ∼28° and 31°, respectively. Such hydrophilicity can be transformed to hydrophobicity by incorporating a low surface energy material like stearic acid. A smooth coating of stearic acid (from 5 wt%) showed a WCA of 76°. The amount of stearic acid added to the precursors was optimized and used throughout the study (5 mL, 5 wt%). Figure 4 shows the effect of precursor concentrations on WCA. It clearly shows that, as the concentration of ZnN or ZnA was increased, there was an increase in WCA. A higher WCA of 155° was obtained for the coatings prepared from 0.3 M ZnA compared to the WCA of 150° obtained from 0.3 M ZnN precursor. Therefore at higher concentrations, coatings from both the precursors exhibit superhydrophobicity. It is interesting to note that at lower precursor concentration of 0.025 M, superhydrophobic coating was obtained from ZnA (WCA 152°), whereas a hydrophobic coating was obtained from ZnN (WCA 132°) precursor. Superhydrophobicity requires a unique combination of micro-nano surface roughness and low surface energy. Even though stearic acid is a low surface energy material, it alone cannot impart superhydrophobicity. Obviously, the micro-nano surface roughness created by the precursors is also responsible for the superhydrophobicity.

The surface morphology of the coatings prepared from different precursors was observed by FESEM. Figure 5(a) shows the microstructure of the coating formed from 0.3 M ZnA, and it was essentially a uniform array of dense microparticles akin to flowers having closed petals. The diameter of the flowers formed was in the range of 5–10 μm. The inset of Fig. 5(a) shows a magnified image of one such flower. The petal of the flower resembled hexagonal flake with length and diameter almost equal to 1 μm. It has also been reported in the literature that the morphology of the zinc oxide crystals formed from chemical bath was affected by the reaction temperature, and flower-like morphology was obtained at a lower temperature [17]. Figure 5(b) represents the microstructure of the coating prepared from 0.3 M ZnN solution, which shows a random mixture of irregular flower and leaf-like structures.

Since the coatings prepared from zinc acetate were superhydrophobic even with lower precursor concentration (0.025 M), the surface morphology of these coatings was analyzed to account for the WCAs. Figure 6(a) shows the surface morphology of the coating obtained from zinc acetate at lower precursor concentration.
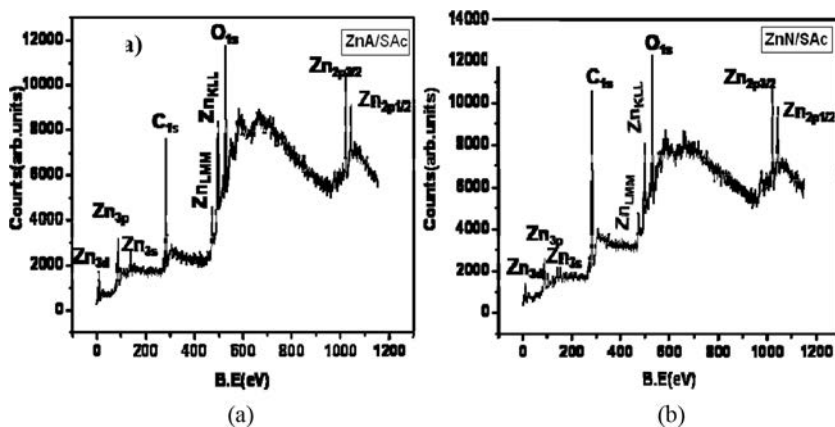

FIGURE 1.—XRD patterns of zinc stearate coatings from 0.3 M precursor concentration.

FIGURE 2.—XPS spectra of coating prepared from (a) 0.3 M ZnA and (b) 0.3 M ZnN.

Flower-like structures with diameter ranging from 5 to 25 µm were formed. Each flower consisted of a number of petals, tapering at the end with diameter less than 1 µm and length almost 3 µm. The coating exhibited a WCA of 152° and a SA less than 2°. Figure 6(b) shows the FESEM images of the coatings prepared from 0.025 M ZnN precursor. The WCA of the coating prepared from ZnN precursor was 132°. The flowers in this case were different from the ones formed from zinc acetate precursor. The diameter of each flower was about 10 µm. The numbers of individual flowers were less and the space between each flower was filled with petal-like structures of diameter 2 µm, and hence the WCA was less compared to the ones prepared from zinc acetate. To examine the role of stearic acid in influencing the morphology of zinc stearate flowers, two control samples were prepared from zinc acetate and zinc nitrate precursors without stearic acid. Figure 7(a) illustrates FESEM images of the coatings prepared from 0.025 M ZnN and 7(b) shows the images of coatings prepared from 0.025 M ZnA solution without stearic acid. Micron-sized flowers were absent in both the coatings and instead oblate

structures with diameter less than 10 µm were formed in the coating prepared from zinc acetate solution (inset 7(b)). The formation of zinc oxide oblate structures from an alkaline zinc acetate solution has been previously reported by Sun et al. [18]. In the absence of stearic acid,

TABLE 1.—Contact angle, sliding angle, and drop profile of the zinc stearates coatings.

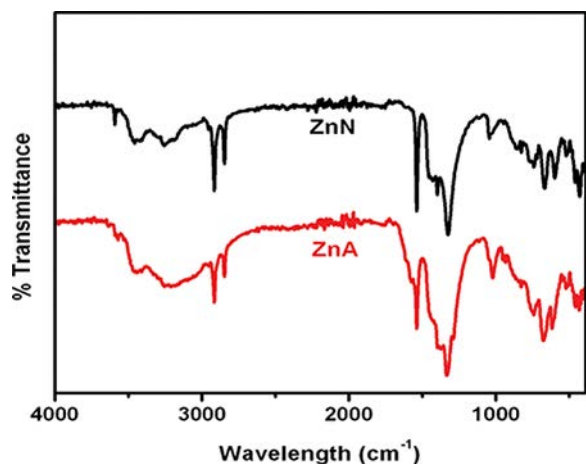| Coatings with	Drop profile	WCA	Sliding angle
1) Stearic acid alone		76°	>90°
2) ZnN alone		31°	>90°
3) ZnA alone		28°	>90°
4) 0.3 M ZnN/SAc		150°	4°
5) 0.3 M ZnA/SAc		155°	<2°
6) 0.025 M ZnN/SAc		132°	37°
7) 0.025 M ZnA/SAc		152°	<2°

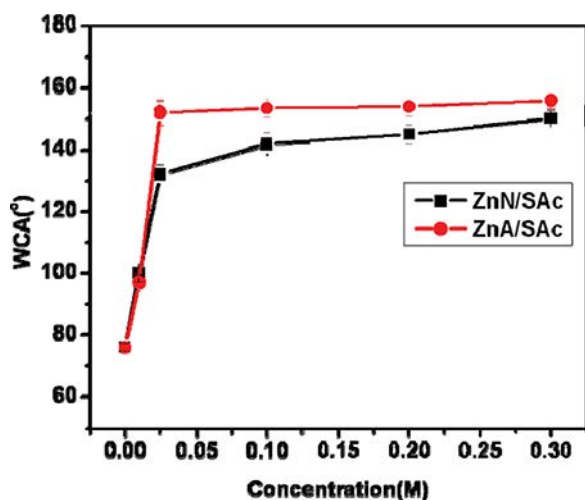FIGURE 3.—FTIR spectra of superhydrophobic zinc stearate coatings from ZnA and ZnN precursors.
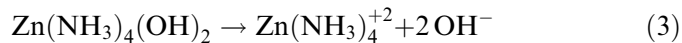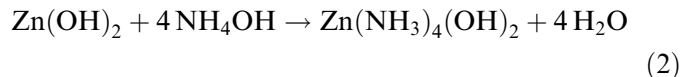
FIGURE 4.—Effect of precursor concentration on WCA for the coatings obtained from ZnA and ZnN.

the coatings prepared from both the precursors were hydrophilic with WCA of 28° and 31°, respectively, for zinc acetate and zinc nitrate precursors. Thus, apart from imparting a low surface energy to the coating, stearic acid may be influencing the morphology of zinc stearate flowers to some extent.

A probable reaction mechanism for the formation of zinc stearate flowers is proposed based on the observations made during the preparation. It was observed that by the addition of NH_4OH to an ethanolic solution of $Zn\,(CH_3COO)_2 \cdot 2H_2O$ a curd-like white precipitate was formed which dissolved in excess of NH_4OH. The precipitate was due to the formation of $Zn\,(OH)_2$ according to the reaction:

$$Zn(CH_3COO)_2 + 2\,NH_4OH \rightarrow Zn(OH)_2$$
$$+ 2\,CH_3COONH_4 \qquad (1)$$
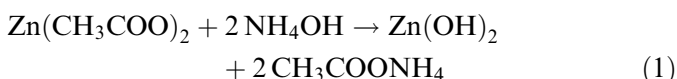
Addition of excess NH_4OH to the solution facilitates the dissolution of $Zn\,(OH)_2$, resulting in the formation of tetra ammonium zinc hydroxide at pH 10

$$Zn(OH)_2 + 4\,NH_4OH \rightarrow Zn(NH_3)_4(OH)_2 + 4\,H_2O$$
$$(2)$$

$$Zn(NH_3)_4(OH)_2 \rightarrow Zn(NH_3)_4^{+2} + 2\,OH^- \qquad (3)$$

Since the reaction is taking place in an open beaker, excess ammonia can escape resulting in the formation of zinc oxide. Li et al. have demonstrated that ZnO formation from basic solutions of zinc acetate by forced hydrolysis is facilitated by the use of open baths [19]. Thus, ZnO particles are formed by forced hydrolysis of $Zn\,(NH_3)_4^{+2}$ in the open bath prior to the reaction with stearic acid as depicted by the reaction.

$$Zn(NH_3)_4^{+2} + 2\,OH^- \rightarrow ZnO + 4NH_3 + 2H_2O \qquad (4)$$
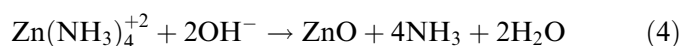
The so-formed ZnO crystals in their hexagonal form have both polar (001) and nonpolar faces (101) parallel to the c-axis. Dipoles of positively charged Zn^{2+} and negatively charged O^{2-} are present on the polar faces. The polar face is thermodynamically less stable than those of other nonpolar faces and tends to grow along c-axis [20]. However, in the present study, since there are different kinds of ions present in the reaction system (i.e., acetate/stearate and OH^- in case of zinc acetate precursor solution and nitrate/stearate and OH^- in case of zinc nitrate precursor solution), it is necessary to explore the functions of these groups in the development of the flower-like morphology. It is reported that excess of CH_3COO^-, NO_3^-, and OH^- ions limit the growth along the c-axis and results in the formation of plate like petals [21, 22]. The positively charged Zn^{2+} of zinc oxide reacts with stearate ion to form zinc stearate. The formation of flower-like particles can be attributed to twinning and fourling growth [23].
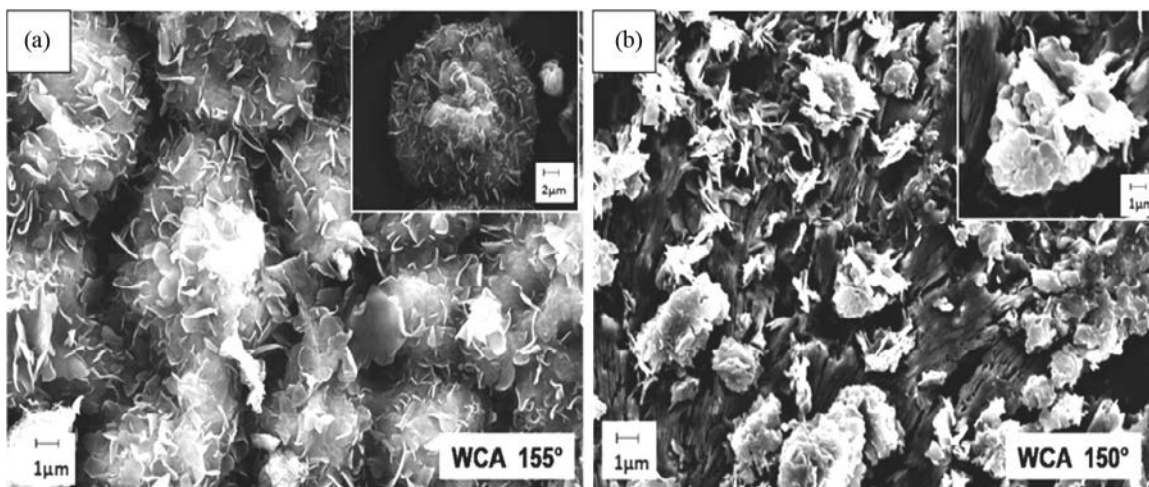

FIGURE 5.—FESEM images of zinc stearate flowers prepared from (a) 0.3 M ZnA, (b) 0.3 M ZnN at magnification 8 K × (inset 25 K ×).
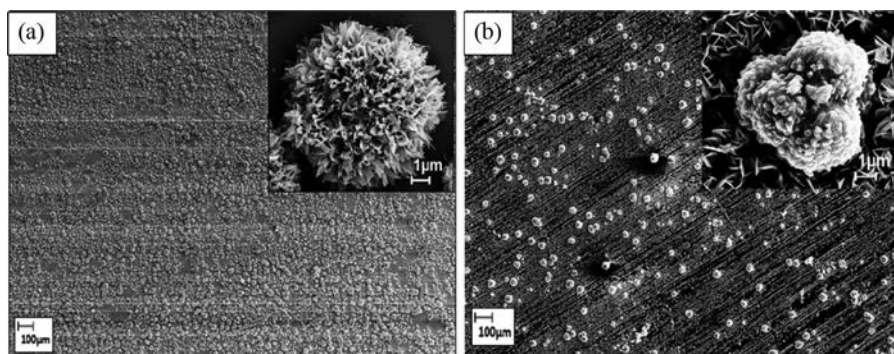
FIGURE 6.—FESEM images of zinc stearate flowers prepared from (a) 0.025 M ZnA and (b) 0.025 M ZnN at magnification 350 × (inset 11 K ×).

Wenzel and Cassie Baxter model has been used to explain the influence of surface roughness on wettability. According to Wenzel model, the liquid drop completely penetrates the surface and wets the surface. According to Casssie Baxter model, the water drop sits on the hills and valleys of the surfaces without wetting it. A superhydrophobic behavior is generally explained in terms of the Cassie–Baxter model [24], according to which,

$$\cos\theta_c = f_1(\cos\theta_e + 1) - 1 \qquad (5)$$

where θ_c is apparent WCA and θ_e is the equilibrium WCA. f_1 is the surface area fraction of the solid.

The coatings prepared from 0.3 M ethanolic precursor solutions (ZnA and ZnN) with stearic acid were superhydrophobic and are in Cassie's state. The surface area fraction of the solid f_1 of the coatings can be calculated using the following equation.

$$f_1 = \frac{(\cos\theta_c + 1)}{(\cos\theta_e + 1)} \qquad (6)$$

The flat smooth coatings of stearic acid obtained showed a WCA (θ_e) of 76°. By substituting the values of θ_e and θ_c (observed WCA) in Eq. (6), f_1 was calculated for the coatings obtained from different precursors at higher (0.3 M) and lower (0.025 M) precursor concentration. The surface area fraction of air trapped between the zinc stearate flowers and the water droplet (f_2) can

also be calculated as $f_2 = 1 - f_1$. The lowest f_1 value of 0.0754 and 0.0942 was obtained for the zinc stearate coatings formed from 0.3 M and 0.025 M zinc acetate precursor solution having flower-like morphology. The corresponding surface area fraction of air trapped under the water drop in contact with flower-like structure for 0.3 M and 0.025 M ZnN (f_2) was 0.1078 and 0.2663, respectively. It has to be noted that a decrease in f_1 indicates an increase in surface roughness. The f_1 value was high (0.2663) for the microstructures formed from the zinc nitrate precursor at lower concentration (0.025 M). This may be attributed to the presence of less number of flower-like structures formed with zinc nitrate precursor. Thus, a water drop on the zinc stearate surface formed from zinc acetate precursor only contacts the tips of the clusters and flower-like structures, resulting in a large water–air interface. Such composite surface prevents water droplets from penetrating into the cavities, thus leading to superhydrophobicity.

CONCLUSIONS

- Zinc stearate superhydrophobic hierarchical surfaces were prepared from ethanolic solution of zinc acetate/zinc nitrate by the addition of stearic acid.
- The coatings obtained from zinc acetate precursor showed superhydrophobicity with WCA >150° even at lower concentration of zinc acetate precursor.
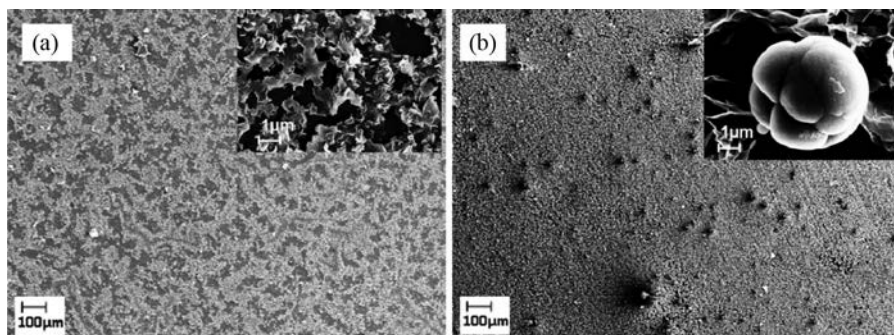

FIGURE 7.—FESEM images of coatings prepared from (a) 0.025 M ZnN at magnification 350 × (inset 11 K ×) and (b) 0.025 M ZnA at magnification 350 × (inset 19 KX) without stearic acid.

- XRD, XPS, and FTIR studies confirmed the formation of zinc stearate.
- The hydrophobicity of the films can be tuned and controlled by the nature and concentration of precursors.
- The surface morphology of the coatings formed from zinc acetate and zinc nitrate precursors were different as evident from FESEM.
- The surface area fraction of air trapped inside the micronano surface was evaluated and found to be higher for the surfaces obtained from zinc acetate precursor (f_2 was 0.948).
- The superhydrophobicity was achieved by the synergistic effect of surface roughness and low surface energy of stearic acid.
- This study clearly shows that zinc acetate is a preferred precursor for the fabrication of superhydrophobic surfaces.
- The present work not only demonstrated a facile route for the preparation of zinc stearate hierarchical micro/ nanostructures, but also provides a very easy method to fabricate superhydrophobic coatings in less time.

REFERENCES

1. Huang, Y.F.; Huang, C.; Zhong, Y.L.; Yi, S.P. Preparing superhydrophobic surfaces with very low contact angle hysteresis. *Surface Engineering* **2013**, *29*, 633–636.
2. Zhang, H.; Lamb, R.N. Superhydrophobic treatment for textiles via engineering nanotextured silica/polysiloxane hybrid material onto fibres. *Surface Engineering* **2009**, *1*, 21–24.
3. Wang, R.G.; Kaneko, J. Hydrophobicity and corrosion resistance of steels coated with PFDS film. *Surface Engineering* **2013**, *29*, 255–263.
4. Xu, Q.F.; Wang, J.N.; Sanderson, K.D. Organic-inorganic composite nanocoatings with superhydrophobicity, good transparency, and thermal stability. *ACS Nano* **2010**, *4*, 2201–2209.
5. Ma, M.R.; Hill, M. Superhydrophobic surfaces. *Current Opinion in Colloid & Interface Science* **2006**, *11*, 193–202.
6. Barthlott, W.; Neinhuis, C. Characterization and distribution of water-repellent, self-cleaning plant surfaces. *Annals of Botany* **1997**, *79*, 667–677.
7. Badre, C.; Mayaffre, A.; Letellier, P.; Turmine, M. Modification of the wettability of a polymeric substrate by pH effect: determination of the surface acid dissociation constant by contact angle measurements. *Langmuir* **2006**, *22*, 8424–8430.
8. Jun, Wu.; Jing Chen.; Jun Xia.; Wei Lei.; Bao-ping Wang. A brief review on bioinspired ZnO superhydrophobic surfaces: theory, synthesis, and applications. *Advances in Materials Science and Engineering* **2013**, Article ID 232681.
9. Sanjay, S.L.; Annaso, B.G.; Chavan, S.M.; Rajiv, S.V. Recent progress in preparation of superhydrophobic surfaces: A review. *Journal of Surface Engineered Materials and Advanced Technology* **2012**, *2*, 76–94.
10. Wang, S.; Feng, L.; Jiang, L. One-step solution-immersion process for the fabrication of stable bionic superhydrophobic surfaces. *Advanced Materials* **2006**, *18*, 767–770.
11. Huang, Y.; Sarkar, D.K.; -Grant Chen, X. A one-step process to engineer superhydrophobic copper surfaces. *Materials Letters* **2010**, *64*, 2722–2724.
12. Li, J.; Wan, H.; Ye, Y.; Zhou, H.; Chen, J. One-step process for the fabrication of superhydrophobic surfaces with easy repairability. *Applied Surface Science* **2012**, *258*, 3115–3118.
13. Capelle, H.A.; Britcher, L.G.; Morris, G.E. Sodium stearate adsorption onto titania pigment. *Journal of Colloid Interface Science* **2003**, *268*, 293–300.
14. Chakradhar, R.P.S.; Kumar, V.D. Water-repellent coatings prepared by modification of ZnO nanoparticles. *Spectrochimica Acta A* **2012**, *94*, 352–356.
15. Wang, S.; Shi, J.; Liu, C.; Xie, C.; Wang, C. Fabrication of a superhydrophobic surface on a wood substrate. *Applied Surface Science* **2011**, *257*, 9362–9365.
16. Gurav, A.B.; Latthe, S.S.; Vhatkar, R.S.; Lee, J.-G.; Kim, D.-Y.; Park, J.-J.; Yoon, S.S. Superhydrophobic surface decorated with vertical ZnO nanorods modified by stearic acid. *Ceramic International* **2014**, *40*, 7151–7160.
17. Wang, Z.; Qian, X.-F.; Yin, J.; Zhu, Z.-K. Large-scale fabrication of tower-like, flower-like, and tube-like ZnO arrays by a simple chemical solution route. *Langmuir* **2004**, *20*, 3441–3448.
18. Sun, L.; Shao, R.; Chen, Z.; Tang, L.; Dai, Y.; Ding, J. Alkali-dependent synthesis of flower-like ZnO structures with enhanced photocatalytic activity via a facile hydrothermal method. *Applied Surface Science* **2012**, *258*, 5455–5461.
19. Li, W.J.; Shi, E.W.; Zhong, W.Z.; Yin, Z.W. Growth mechanism and growth habit of oxide crystals. *Journal of Crystal Growth* **1999**, *203*, 186–196.
20. Govender, K.; Boyle, D.S.; Kenway, P.B.; Brien, P.O. Understanding the factors that govern the deposition and morphology of thin films of ZnO from aqueous solution. *Journal of Materials Chemistry* **2004**, *14*, 2575–2591.
21. Zhang, D.; Sun, L.; Zhang, J. Hierarchical construction of ZnO architectures promoted by heterogeneous nucleation. *Crystal Growth and Design* **2008**, *8*, 3609–3615.
22. Yu, Q.; Yu, C.; Yang, H.; Fu, W.; Chang, L.; Xu, J.; Wei, R.; Li, H.; Zhu, H.; Li, M.; Zou, G. Growth of dumbbell-like ZnO microcrystals under mild conditions and their photoluminescence properties. *Inorganic Chemistry* **2007**, *46*, 6204–6210.
23. Gao, X.; Li, X.; Yu, W. Flowerlike Zno nanostructures via hexamethylenetetramine-assisted thermolysis of zinc–ethylenediamine complex. *Journal of Physical Chemistry B* **2005**, *109*, 1155–1161.
24. Cassie, A.B.D.; Baxter, S. Wettability of porous surfaces. *Transactions of the Faraday Society* **1944**, *40*, 546–551.